Journal of Radiation Research and Applied Sciences 8 (2015) 142–147

HOSTED BY

Available online at www.sciencedirect.com
ScienceDirect
Journal of Radiation Research and Applied Sciences
journal homepage: http://www.elsevier.com/locate/jrras

Seasonal behavior of radon decay products in indoor air and resulting radiation dose to human respiratory tract

A.M.A. Mostafa [a,*], H. Yamazawa [b], M.A.M. Uosif [a], J. Moriizumi [b]

[a] Physics Department, Faculty of Science, Al-Azhar University, Assiut Brunch, Assiut 71542, Egypt
[b] Graduate School of Engineering, Nagoya University, Furo-cho, Chikusa-ku, Nagoya 464-8603, Japan

ARTICLE INFO

Article history:
Received 18 November 2014
Received in revised form
17 December 2014
Accepted 22 December 2014
Available online 2 January 2015

Keywords:
Activity size distribution
Radon
Radon progenies
Lung dose

ABSTRACT

Most of radiation hazard of indoor radon is largely due to the radon progenies, which are inhaled and deposited in the human respiratory tract. It is essential to evaluate aerodynamic characteristics of the radon progenies, which are either attached or unattached to aerosol particles, because the dose is strongly dependent on the location of deposition in respiratory tract and hence on the aerodynamic characteristics of the aerosol particles. This paper presents the seasonal behavior of radon decay products in indoor air under domestic conditions at Nagoya University, Japan. A low pressure cascade impactor as an instrument for classifying aerosol sizes and imaging plate as a radiation detector have been employed to characterize the activity size distribution of short-lived radon decay products. In parallel, radon and its progenies concentrations were measured. Taking into account the progeny characteristics, the inhalation dose in the different seasons was also estimated based on a lung dose model with the structure that is related to the ICRP66 respiratory tract model. The result evident that, the highest dose 0.22 $mSvy^{-1}$ was observed during the winter where the highest value of equilibrium equivalent concentration of radon (EEC) and lowest value of the activity median aerodynamic diameter (AMAD) were found in this season; whereas, the dose in spring appeared to be lowest 0.02 $mSvy^{-1}$.

1. Introduction

The natural radioactive gas ^{222}Rn generated in the Earth's crust by the ^{238}U series, It's concentration levels depend strongly on geological and geophysical conditions, as well as on atmospheric influences such as barometric pressure. Radon escapes from the ground and accumulates in rooms according to the strength of its emanation and its dilution by ventilation (Hopke, 1992). High radon concentration in indoor air, in addition to long exposure periods related to indoor habitation, makes indoor radon a potential hazard (Marcinowski, 1992). Once in the atmosphere, the ^{222}Rn atoms decay producing short-lived (^{218}Po, ^{214}Pb, ^{214}Bi, ^{214}Po) and longlived (^{210}Pb, ^{210}Bi, ^{210}Po) radioactive decay products. Most of these radionuclides can be adsorbed on the surface of the

* *Corresponding author.*
E-mail address: ah_elsaih@yahoo.com (A.M.A. Mostafa).
Peer review under responsibility of The Egyptian Society of Radiation Sciences and Applications.
http://dx.doi.org/10.1016/j.jrras.2014.12.007

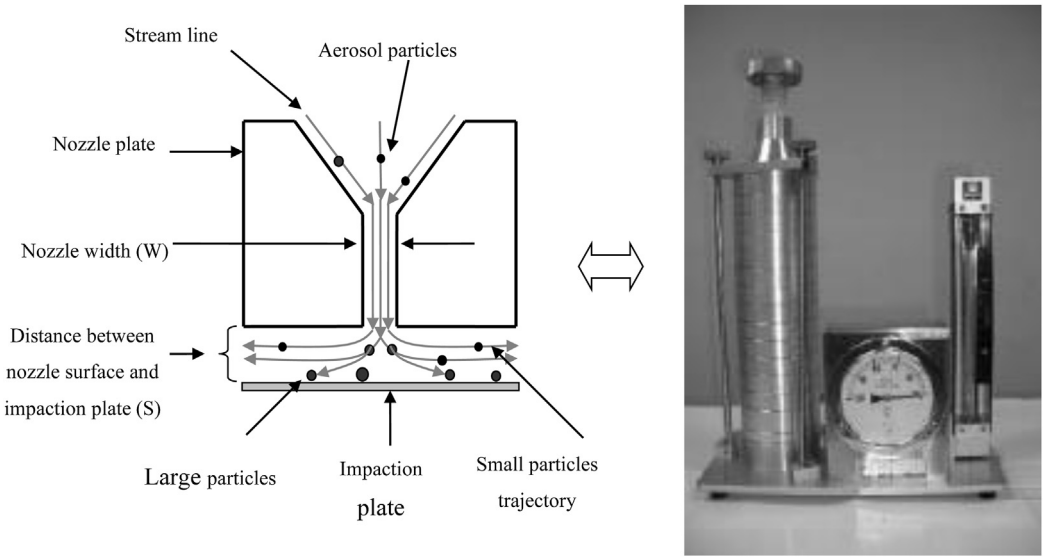

Fig. 1 – The low pressure cascade impactor with the schematic representation of a stage within impactor.

existing aerosol particles always present in various concentrations in the ambient air forming the radioactive aerosol of the radon progeny and their fate will follow that of the carrier aerosols (Mostafa, Tamaki, Moriizumi, Yamazawa, & Iida, 2011). The airborne radon decay products deposit in human respiratory tract by inhalation and damage the sensitive tissues of respiratory tract. Thus the inhaled radon decay products are determined to be the second leading cause of lung cancer after tobacco smoking (Frumkin & Samet, 2001). Knowing the size distribution of radon progeny aerosols is an important parameter needed for estimating the human lung dose with regard to radiation protection. The deposition of radon progeny in the human respiratory tract can be estimated more exactly if its size distribution is known (Shimo, Torii, & Ikebe, 1981). Atmospheric aerosol size distribution basically consists of three separate modes. Nucleation mode (particles smaller than 0.1 mm), accumulation mode (particles between 0.1 and 1 mm) and coarse mode (particles larger than 1 mm) (Camacho, Valles, Vargas, Gonzalez-Perosanz, & Ortega, 2009). For a few years following development of a suitable device, more detailed size distributions of radon progeny have been measured by several researchers (Becker, Reineking, Scheibel, & Porstendorfer, 1984; Hopke et al., 1992; Mohamed, Abd El-hady, Moustafa, Yuness, 2014; Reineking, Becker, & Porstendorfer, 1988; Tu, Knutson, & George, 1991; Wasiolek & Cheng, 1995). The aerosols behavior differs depending on many factors. The physical properties of aerosols are affected by particle size, shape, and density. Ambient humidity can be particularly important, as hygroscopic particles will increase in size as they flow through a moist airstream. The seasonal change can be recognized as one of the variation factors which influence the aerosols behavior. Therefore, in the present study, the seasonal variations of activity size distribution, radon and its progeny concentration, and the effective dose due to inhalation of radon and its decay products in indoor environment were estimated at Nagoya university, Japan. The climate of Nagoya, where the experiments were conducted, is typified with warm spring, a lasting rainy season followed by humid but less rainy summer, relatively mild autumn with rather periodic rains and slightly cool winter with occasional snowfalls. The measurements were carried out during the five seasons at one specific location. Despite that the rain falls more heavily during the rainy season, but there may be some intermittent rainy days during the other seasons.

2. Materials and methods

2.1. *Measurement conditions*

The experimental site was a laboratory room, located in 5th floor in new multi-storied building, the room volume is about 200 m^3 with composite structure of concrete and steel, with two entering doors and one large wall to-wall glass windows. The measurements were carried out under normal conditions in the laboratory room i.e. sometimes doors and/or windows were open. The air conditioner was stopped during sampling time to exclude the air conditioning affects on the concentrations and behaviors of radon, radon progeny, and aerosol particles. The human activities were kept as a minimum as possible during the measurement periods. All the instruments employed in this study were placed at the centre of room and one meter above the ground during performing. The measurement was conducted during the period from June, 2009 to July, 2010, the experimental period was divided in to five segments by defining as the seasons. Spring was defined as the period from March to May; rainy season from late June to July, summer from late July to August, autumn from September to November, and winter from December to February. At least five measurements were carried out for each season. The measurements were performed during the typical Japanese working hours i.e. from 9:00 am to 5:00 pm.

2.2. Instruments description

2.2.1. The impactor

The radon aerosol-particle size distribution was measured employing an Andersen low pressure cascade impactor (LP-20RPS47, Tokyo Dylec Co. Ltd.). It is a round multijet, multi-stage impactor having 12 size fractionating stages and one back-up filter holder, and operated at a flow rate of 25.7 l min21 with a reduced pressure of 273.3 kPa at the last stage (Fig. 1). The aerodynamic cut-off diameters, corresponding to particle diameter collected with the efficiency of 50% are evaluated with the theoretical calculation to be 12.0, 8.1, 5.5, 3.5, 1.9, 1.0, 0.73, 0.48, 0.28, 0.19, 0.11 and 0.05 mm. The smaller particles are collected by the backup filter in the last stage. The air sample was collected on 47 mm diameter of stainless steel plates. Each detecting surface was uniformly coated with a thin layer of silicon grease (Dow Corning Co. Ltd.) to prevent particle bounce-off. The unattached particles were separated at the entrance of impactor using wire screen mesh # 635.

2.2.2. The imaging plate (IP)

The imaging plate (IP) employed in the study is BAS-SR (20 cm × 25 cm, Fuji Film Co. Ltd). It is a two-dimensional image sensor with a linear response, high sensitivity and wide dynamic range to radiation (Sakoda et al., 2010). The IP is composed of a flexible plastic plate coated with fine crystals (grain size: about 5 μm) of photo-stimulable phosphor of barium fluorobromide containing a trace amount of bivalent europium as a luminescence center, formulated as BaFBr: Eu^{2+} combined with an organic binder. The composite structure of the imaging plate is shown in (Fig. 2). Alpha radiation emitted by radon progeny incident to the crystal creates holes and electrons: the former allow Eu^{2+} ions to become Eu^{3+} ions and the latter are trapped at $F(Br^-)$ or $F(F^-)$ centers. Through this process the photostimulable phosphor can store a fraction of the energy from absorbed incident radiation. The exposed imaging plate is scanned with a laser beam of red light through the image reader provides the necessary energy to release the trapped charges and Eu^{3+} ions are recombined to make excited Eu^{2+} ions. Subsequently, they emit photo-stimulated luminescence (PSL). Information on the deposited radiation energy is obtained by reading out the PSLs by the image reader. The irradiated IP can be repeatedly refreshed by exposure uniformly to visible light, which can erase the stored radiation image in the phosphor.

2.3. Experimental procedure

The aerosol collection time was 60 min, and cooling time was 20 min. The cooling time was set long enough to allow ^{218}Po to decay (half-life is 3.05 min). Afterwards, all the collection mediawere placed onto an imaging plate (IP) cassette to keep in a close contact with the IP and allowed to have a radiation exposure for the next successive 60 min. A bio-imaging analyser by the Fuji Film Company Limited (BAS-5000) was used as image reader. The alpha spot images on the IP were counted by a computer program (Rahman et al., 2007) Radon concentration was continuously measured with a pulse-type ionization chamber (AlphaGUARD, manufactured by Genitron Instruments, Germany). The equilibrium equivalent concentration (EEC) was continuously measured using a working level measurement system (Pylon Electronics Inc., Model 147 Colonnade Road, Ottawa, Ontario, Canada). Li-840 CO2/H2O Gas Analyzer, and lAQ monitor (KANOMAX) were employed to characterise air exchange by comparison of carbon dioxide concentration indoor and outdoor.

3. Result and discussion

3.1. Seasonal variation of activity size distribution

The particle size distributions of radon progeny aerosols were described in terms of a log–normal distribution, defined by the activity median aerodynamic diameter (AMAD) and geometric standard deviation (σ_g) inscribing the frequency function 'f' using the following equation (Eq. (1)) (Hinds, 1982):

$$df = \frac{1}{\sqrt{2\pi}\ln \sigma_g}\exp\left[-\frac{(\ln d_p - \ln AMAD)^2}{2(\ln \sigma_g)^2}\right] d\ln d_p \quad (1)$$

Where d_p is the particle diameter, AMAD is the median diameter and σ_g is the geometric standard deviation.

Fig. 3 illustrates the variations of activity size distribution parameters (AMAD and σ_g) in the five different seasons around the year. The obtained data are listed also in (Table 1). Form the obtained results it can be observed that the highest

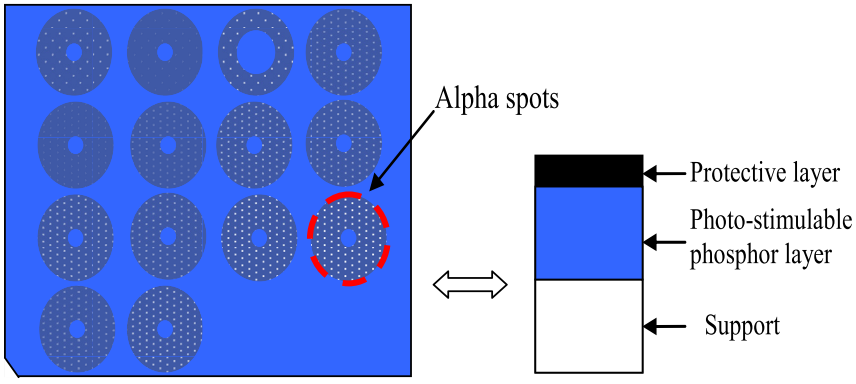

Fig. 2 – The surface and cross-sectional view of imagine plate.

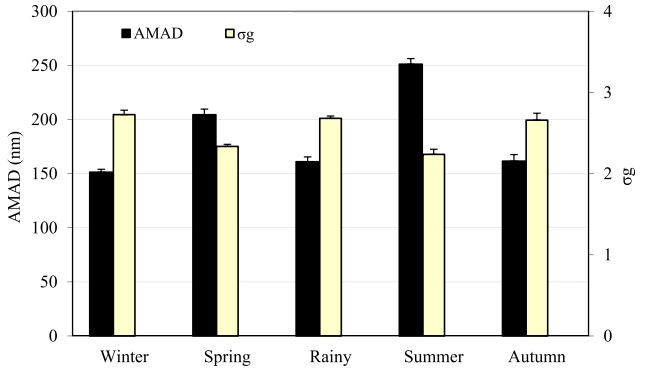

Fig. 3 – The seasonal variations of AMAD (nm) and σg values.

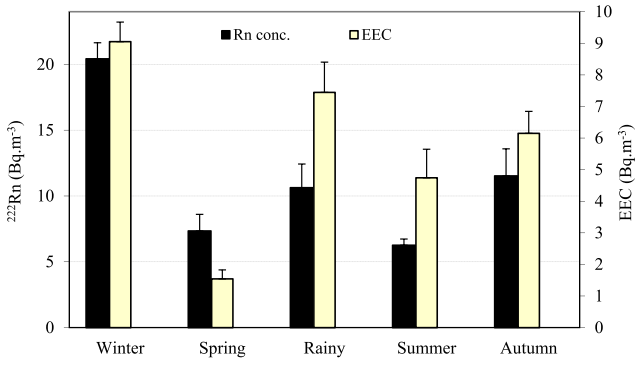

Fig. 4 – The seasonal variations of ^{222}Rn (Bq m^{-3}) and EEC (Bq m^{-3}) values.

value of AMAD was 251.13 nm which obtained during the summer and the lowest 151.4 nm was obtained during the winter. Conversely, the highest value of σ_g 2.73 was obtained during the winter and the lowest 2.42 was obtained during the summer season. For spring, autumn, and rainy seasons the obtained values were 204.5, 161.1, and 161 nm respectively for AMAD values and 2.34, 2.66, and 2.68 respectively for σ_g values. Apossible explanation is as follows. Warm air can hold more moisture than cold air. As well, the fine particles which constitute most of atmospheric aerosol result almost entirely from vapor condensation and coagulation. Then during the summer, the high temperature of the earth builds up of natural radioactive aerosol particles with larger AMAD and also leads to decrease the size range of the radioactive aerosol particles to be more close to a monodisperse aerosol which mean decrease in σ_g values. On the other hand, the reverse process is applicable for the cold air in winter and thus providing lower value of AMAD and higher value of σ_g in winter season.

3.2. *Seasonal variation of radon and its progeny*

The radon concentration indoors is mainly influenced by the strength of sources and the air exchange with the outdoor air. Both parameters can change with meteorological parameters (wind speed, indoor–outdoor temperature pressure difference), with activities of the inhabitants, mechanical ventilation and heating systems. Thus it is difficult to describe the seasonal variation phenomenon of indoor radon concentration. However, it has been reported that the cold seasons show higher radon concentrations in dwelling houses than the warm seasons (Papastefanou, Stoulos, Manolopoulou, Ioannidou, & Charalambous, 1994). In the current study, the seasonal variation of indoor radon and its decay products (equilibrium equivalent concentration "EEC") concentrations (Bq m^{-3}) were monitored and the results are presented in Fig. 4. The obtained result indicates that, the highest value of radon concentration was 20.42 Bq m^{-3} obtained in winter and the lowest value was 6.26 Bq m^{-3} obtained in summer season. The mean value of radon concentration in the other seasons was 11.52, 10.63, and 7.34 Bq m^{-3} for autumn, rainy season, and spring seasons respectively. The highest value of EEC was 9.05 Bq m^{-3} obtained in winter too and the lowest was 1.54 Bq m^{-3} registered in the spring season. For rainy season, autumn and summer the obtained values of EEC were 7.45, 6.15, and 4.74 Bq m^{-3}, respectively. The high values of radon and its decay products concentration in winter are because of poor ventilation as the doors and windows of the experimental room remain closed most of the time. Whereas, the high ventilation in spring season where the windows are kept open more frequently and for more duration seems to have led to the low values of radon and its decay products concentration in the spring season. Although the ventilation rate is presumably reduced also during the rainy season, but the values of radon and its decay products concentration remain moderate which may be attributed to the low emanation of radon from the mineral grains due to the presence of more moisture. The results in this study are based only on short-term measurements. However, the concentration of radon in a building is highly variable as mentioned above. Thus, these short-term measurements may not provide an adequate estimate of the average indoor concentration. Also, in most

Table 1 – The mean values of AMAD (nm), σ_g, radon concentration (Bq m^{-3}), EEC (Bq m^{-3}), and effective dose (mSvy^{-1}) in the five seasons at site B.

Season	AMAD (nm)	σ_g (–)	Rn conc. (Bq m^{-3})	EEC (Bq m^{-3})	Effective dose (mSvy^{-1})
Winter	151.4 ± 2.6	2.7 ± 0.05	20.4 ± 1.2	9.1 ± 0.6	0.22 ± 0.02
Spring	204.5 ± 5.2	2.3 ± 0.03	7.3 ± 1.3	1.5 ± 0.3	0.02 ± 0.001
Rainy	161 ± 4.5	2.7 ± 0.03	10.6 ± 1.8	7.4 ± 1	0.17 ± 0.02
Summer	251.1 ± 5.2	2.2 ± 0.06	6.3 ± 0.5	4.7 ± 0.9	0.07 ± 0.02
Autumn	161.6 ± 5.9	2.7 ± 0.08	11.5 ± 2.1	6.2 ± 0.7	0.14 ± 0.01

cases, the concentration of radon is low so that a long counting interval may be needed to obtain sufficient statistical precision in the total a count.

3.3. *Seasonal variation of effective dose*

The estimated values of AMAD, σ_g, and EEC were input into a commercially available lung dose calculation program (LUDEP 2.0), which runs the ICRP 66 human respiratory tract model (HRTM), to determine the effective dose. This model contains several built-in databases, including radionuclide decay data from Oak Ridge National Laboratory and from ICRP-38; biokinetic models from ICRP-30; and bioassay functions from ICRP-54. ICRP data are generally used as the default values within the model, although the user is given the option to input case-specific parameters. These input parameters were varied according to their characteristic distributions, in an effort to perform uncertainty analysis of regional deposition fraction. The sensitivity of the weighted equivalent dose to lung per unit exposure of radon decay products to HRTM was verified in many literatures. The parameters considered to be most influential are: (1) aerosol parameter, (2) subject related parameters such as breathing rate, fraction inhaled through nose and age and gender of the subject itself, (3) target cell parameters, and (4) parameters that define the absorption rates of the radon decay products from the lung to the blood. In considering all these sensitive parameters, best estimated input parameter values were taken for LUDEP to calculate the dose for the present study and these values are presented in Table 2. These parameter values are the best representation for radon decay products measured at indoors and were recommended by Marsh and Birchall (2000) and Ishikawa, Tokonami, Yonehara, Fukutsu, and Yamada (2001). The best estimated parameter values used for the lung model are HRTM default values for a male adult at indoor environment.

As mentioned before the effective dose depend mainly on radon and its decay products concentrations in addition to the activity size distribution of the short-lived radon daughters. Thus, it is expected that the seasonal variation of the effective dose will follow the variation of these factors. To show the seasonal variation of the effective dose the mean values ($mSvy^{-1}$) are plotted in Fig. 5 for the five different seasons round the year. From the obtained result, it is evident that, the highest dose 0.22 $mSvy^{-1}$ was observed during the winter where the highest value of EEC and lowest value of AMAD were found in this season; whereas, the dose in spring appeared to be lowest 0.02 $mSvy^{-1}$, influenced by the significant reduction of radon and its decay products concentrations. For rainy season, autumn, and summer the dose were estimated to be 0.17, 0.14, and 0.07 $mSvy^{-1}$, respectively. So as expected before, the effective dose fluctuate mainly with the variation of radon and its decay products concentrations, and also with activity size distribution of the short-lived radon daughters. The world average inhalation dose due to radon and its progeny is 1.2 $mSvy^{-1}$as recommended by UNSCEAR (2000), which reveals that the studied area is safe as far as health hazards are concerned.

Table 2 – The best estimated parameter values for the present study.

Description of parameter	Best estimate
Average breathing rate ($m^3.h^{-1}$)	0.78
Particle density (g/cc)	1.0
Particle shape factor	1.0
Equilibrium factor unattached Particle	0.1
Unattached particle size (mm)	0.001
Fraction cleared by rapid Dissolution	1.00
Rapid dissolution rate	1.65

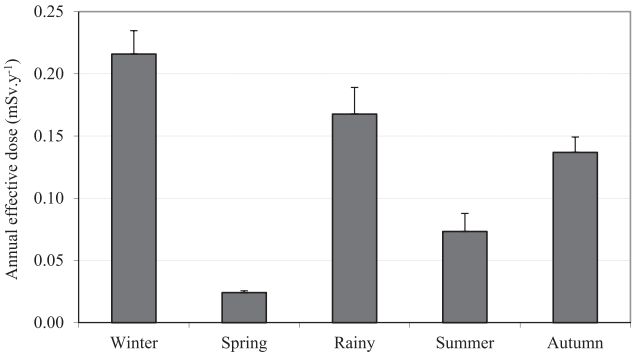

Fig. 5 – The seasonal variations of effective dose ($mSvy^{-1}$).

4. Conclusions

In this research, the seasonal variations of activity size distribution, radon and its progeny concentration, and the effective dose due to inhalation of radon and its decay products were studied, the result concluded that:

- The highest value of AMAD was 251.1 nm which obtained during the summer and the lowest AMAD of 151.4 (nm) was obtained during the winter. Conversely, the highest value of σ_g 2.73 was obtained during the winter and the lowest 2.42 was obtained during the summer season. Since the capacity of the air to hold moisture is proportional to ambient temperature, so during the summer the high temperature of the earth may builds up of natural radioactive aerosol particles with larger AMAD with the reverse process in winter and thus providing lower value of AMAD.
- The highest value of radon concentration was 20.42 Bq m^{-3} obtained in winter and the lowest value was 6.26 Bq m^{-3} obtained in summer season.
- The highest value of EEC was 9.05 Bq m^{-3} obtained in winter too and the lowest value 1.54 Bq m^{-3} was registered in the spring season.
- The high values of radon and its decay products concentration in winter may attribute to the poor ventilation as the doors and windows of the experimental rooms remain closed most of the time and the reverse in summer and spring.
- The highest value of dose 0.22 $mSvy^{-1}$ was observed during the winter where the highest value of EEC and the lowest value of AMAD; whereas the effective doses in spring was evaluated to be the lowest at 0.02 $mSvy^{-1}$, influenced by the significant reduction of radon and its decay products concentrations.

REFERENCES

Becker, K. H., Reineking, A., Scheibel, H. G., & Porstendorfer, J. (1984). Radon daughter activity size distributions. *Radiation Protection Dosimetry, 7*, 147–150.

Camacho, A., Valles, I., Vargas, A., Gonzalez-Perosanz, M., & Ortega, X. (2009). Activity size distributions for long-lived radon decay products in aerosols collected in Barcelona (Spain). *Applied Radiation and Isotopes, 67*, 872–875.

Frumkin, H., & Samet, J. S. (2001). Radon. *CA: A Cancer Journal for Clinicians, 51*(6), 337–344.

Hinds, W. C. (1982). *Aerosol technology properties, behavior, and measurement of airborne particles*. New York: Wiley-Interscience Publication.

Hopke, P. K. (1992). Some thoughts on the unattached fraction of radon decay products. *Health Physics, 63*, 209–212.

Hopke, P. K., Wasiolek, P., Montassier, N., Govallo, A., Gadsby, K., & Socolow, R. (1992). Measurement of activity-weighted size distributions of radon decay products in a normally occupied home. *Radiation Protection Dosimetry, 45*, 329–331.

Ishikawa, T., Tokonami, S., Yonehara, H., Fukutsu, K., & Yamada, Y. (2001). Effects of activity size distribution on dose conversion factor for radon progeny. *Japanese Journal of Health Physics, 36*(4), 329–338.

Marcinowski, F. M. (1992). Nationwide survey of residential radon levels in the US. *Radiation Protection Dosimetry, 45*, 419–424.

Marsh, J. W., & Birchall, A. (2000). Sensitivity analysis of the weighted equivalent lung dose per unit exposure from radon progeny. *Radiation Protection Dosimetry, 87*(3), 167–178.

Mohamed, A., Abd El-hady, M., Moustafa, M., & Yuness, M. (2014). Deposition pattern of inhaled radon progeny size distribution in human lung. *Journal of Radiation Research and Applied Sciences, 7*, 333–337.

Mostafa, A. M. A., Tamaki, K., Moriizumi, J., Yamazawa, H., & Iida, T. (2011). The weather dependence of particle size distribution of indoor radioactive aerosol associated with radon decay products. *Radiation Protection Dosimetry, 146*(1–3), 19–22.

Papastefanou, C., Stoulos, S., Manolopoulou, M., Ioannidou, A., & Charalambous, S. (1994). Indoor radon concentrations in Greek apartment dwellings. *Health Physics, 66*(3), 270–273.

Rahman, N. M., Iida, T., Saito, F., Koarashi, J., Yamasaki, K., Yamazawa, H., et al. (2007). Evaluation of aerosol sizing characteristic of an impactor using imaging plate technique. *Radiation Protection Dosimetry, 123*(2), 171–181.

Reineking, A., Becker, K. H., & Porstendorfer, J. (1988). Measurements of activity size distributions of the short-lived radon daughters in the indoor and outdoor environment. *Radiation Protection Dosimetry, 24*, 245–250.

Sakoda, A., Ishimori, Y., Hanamoto, K., Kawabe, A., Kataoka, T., Nagamatsu, T., et al. (2010). Applicability and performance of an imaging plate at subzero temperatures. *Applied Radiation and Isotopes, 68*, 2013–2015.

Shimo, M., Torii, T., & Ikebe, Y. (1981). Measurements of unattached and attached RaA atoms in the atmosphere and their deposition in human respiratory tract. *Journal of Atomic Energy Society of Japan, 23*, 851–861.

Tu, K. W., Knutson, E. O., & George, A. C. (1991). Indoor radon progeny aerosol size measurements in urban, suburban, and rural regions. *Aerosol Science and Technology, 15*, 170–178.

UNSCEAR. (2000). Sources and biological effects of ionizing radiation. *United Nations Scientific Committee on the effects of atomic radiation, United Nations, New York*.

Wasiolek, P. T., & Cheng, Y. S. (1995). Measurements of the activity-weighted size distributions of radon decay products outdoors in central New Mexico with parallel and serial screen diffusion batteries. *Aerosol Science and Technology, 23*, 401–410.